https://doi.org/10.5194/egusphere-2023-1432
Preprint. Discussion started: 11 July 2023

QBO modulation of the Asian Monsoon water vapour

Cristina Peña-Ortiz[1], Nuria Pilar Plaza[2], David Gallego[1], Felix Ploeger[3,4]

[1]Universidad Pablo de Olavide, Sevilla, 41013, Spain
[2]Centro de Investigaciones sobre Desertificación, Consejo Superior de Investigaciones Científicas (CIDE-CSIC), 46113 Moncada, Valencia, Spain
[3]Institute of Climate Research, Stratosphere (IEK-7). Forschungszentrum Jülich, Jülich, 52428, Germany
[4] Institute for Atmospheric and Environmental Research, University of Wuppertal, Wuppertal, 42119, Germany

Correspondence to: Cristina Peña-Ortiz (cpenort@upo.es)

Abstract. The Asian Monsoon (AM) plays a key role in the transport of water vapour to the lower stratosphere and contributes significantly to the wet phase of the annual global stratospheric water vapour cycle. Although it is known that the QBO is one of the main drivers of the interannual variability of the AM water vapour, the physical mechanisms responsible for this variability remain unclear. Here we have used daily MLS data for the period 2005-2020 to characterize the QBO signature on the lower stratosphere AM water vapour during the boreal summer. We show that the QBO has the strongest impact during August, when QBO-W minus QBO-E differences may reach 1ppmv at 100hPa, although a significant signature is also observed during July. We find that the region whose temperature controls the QBO signal on water vapour over the AM differs between July and August. In July, when the key region is over the tropical Indian Ocean, the QBO modulation of the AM water vapour occurs in phase with the signal over the equator whereas in August, when the key region is at the subtropics, over the southwestern flank of the Monsoon, the signal over the AM is opposite to that over the equator. Our results reveal that the QBO signal on the temperature on the south side of the anticyclone, which ultimately has an impact on AM water vapour, is, in turn, modulated by the QBO impact on convection. Thus, we find that the QBO signature on convection over the equator gives rise to Rossby waves trains that produce variations in convection over the southern side of the AM anticyclone such that weaker convection over this region generates an increase in water vapour and vice versa.

1 Introduction

Almost all of the water vapour in the lower stratosphere appears as a result of transport from the troposphere, with a small additional contribution due to methane oxidation. This transport occurs mainly through the tropical tropopause, often call the "cold trap", where horizontal transport causes air masses to experience extraordinarily low temperatures as they pass through the coldest regions, limiting the water vapour concentration in the lower stratosphere to a few parts per million (Holton and Gettelman, 2001; Fuegistaler et al., 2004, Fueglistaler et al., 2009; Liang et al., 2011; Randel et al., 2004; Zhou et al., 2001, 2004). However, despite its low concentration, water vapour in the lower stratosphere plays a fundamental role in radiative balance in the tropics (Brindley and Harries, 1998) and in the ozone chemistry (Dvortsov and Solomon, 2001; Stenke and Grewe, 2005).

https://doi.org/10.5194/egusphere-2023-1432
Preprint. Discussion started: 11 July 2023

It is generally accepted that monsoon regions play a key role in troposphere-to-stratosphere transport and thus in the concentration of water vapour in the lower stratosphere. In the Northern Hemisphere, stratospheric water vapour concentration shows two maxima between 150hPa and 70hPa over the Asian and North American monsoon regions (Rosenlof et al., 1997; Park et al., 2007). These summer climatological maxima can influence water vapour over much of the Northern Hemisphere through their large-scale transport (Ploeger et al., 2013) and are very likely to contribute significantly to the wet phase of the annual global stratospheric water vapour cycle. In this regard, Nuetzel et al., (2019) showed, through model simulation, that the AM contributes ~15% to tropical tape recorder wet phase, and ~30% to NH extratropical lowermost stratosphere summertime water vapour maximum. Different global models suggest that convection over the Southeast Asian monsoon region represents the major source of moisture to the stratosphere (Bannister et al., 2004).

Despite their importance, there is much uncertainty regarding the physical mechanisms that generate water vapour maxima over monsoon regions. In particular, it is not known how important deep convection, monsoon temperature and circulation, or in situ dehydration of air masses may be. Randel and Park (2006) show consistent fluctuations in deep convection and water vapour content of the Asian monsoon anticyclone. However, on an intraseasonal scale, the peaks in stratospheric water vapour over the monsoons do not coincide either spatially or temporally with the peaks in convective activity, suggesting that horizontal transport may play a role. In fact, and contrary to expectations, Randel et al. (2015) found that deep convection over the Asian and North American monsoons is associated with a drier stratosphere, which they explain through the cooling of the lower stratosphere produced by the convection itself. Thus, their results suggest that, on an intraseasonal scale, stratospheric water vapour over the Asian and North American monsoons is mainly controlled by large-scale temperature variations forced by deep convection. In contrast, other studies suggested a moistening effect of overshooting convection in the Asian monsoon (e.g., Khaykin et al., 2022), but with the impact on the lower stratosphere water vapor budget currently under debate (Konopka et al., 2023).

Lower stratospheric water vapour over the Asian and North American monsoons exhibits very significant interannual variability in which the Quasi-biennial Oscillation (QBO) and ENSO (El Niño Southern Oscillation) appear to dominate (Randel et al., 2015). However, the physical mechanisms responsible for this variability have been poorly investigated, hitherto. In general terms, we know that the concentration of water vapour in the stratosphere is profoundly influenced by global circulation patterns, particularly those affecting the tropical regions, as ENSO and the QBO, through which transport preferentially occurs. The QBO dominates the interannual variability of water vapour in the lower and middle stratosphere by modulating tropical tropopause temperatures and, in spite of the fact that its signal is relatively weak at the tropopause (± 1K), it has a significant influence on the mixing ratio of rising air into the stratosphere (Giorgetta and Bengtsson, 1999; Geller et al., 2002, Tian et al., 2019). However, Randel et al. (2015) found asymmetries in the QBO signal over the Asian and North American monsoons that, a priori, are not consistent with the mechanism based on temperature modulation, since the QBO signal on temperature is zonally symmetric.

https://doi.org/10.5194/egusphere-2023-1432
Preprint. Discussion started: 11 July 2023

In addition, the QBO also influences deep convection processes in the tropics (Giorgetta and Bengtsson, 1999, Peña-Ortiz et al., 2019), determining the other important mechanism in the transport of vapour across the tropopause. Giorgetta and Bengtsson (1999) showed that during the easterly phase of the QBO there is an intensification of convection over the East Asian and Indian monsoons leading to increased cloudiness in areas close to the tropopause. However, the effect of this modulation of convection on the transport of water vapour into the stratosphere has not yet been studied.

In this paper we analize the QBO impact on water vapour in the lower stratosphere over the Asian moonson. We make use of observational data from the Microwave Limb Sounder (MLS) to quantify and describe the behaviour of this signature during July and August according to the QBO phases. Additionally, we examine the QBO signature on temperature and convection and address the question concerning the role that these variables play in the QBO signal on the water vapour over the AM.

2 Data and Methodology

We have analyzed observations of water vapour mixing ratio and temperature in the lower stratosphere from the Microwave Limb Sounder (MLS) aboard the NASA satellite Aura (Waters et al., 2006). For both variables we have used MLS 4.2 version (Lambert et al., 2015, Livesey et al., 2020) from which we have produced gridded daily data on 100hPa and 82 hPa pressure levels by averaging profiles inside bins with resolution of 2° latitude × 5° longitude for the period 2005-2020. Water vapour measurements have been validated in several studies and have been part of a climatological overview of the Asian Monsoon Anticyclone (Santee et al., 2017). The single profile precision of the MLS water vapour is 7% and 15% at 82hPa and 100hPa while accuracy is 9% and 8% respectively for these two pressure levels (Table 3.9.1 of Livesey et al. (2020). The single profile precision and accuracy of the MLS temperature data product are shown in Table 3.22.1 of Livesey et al. (2020). The precision is 0.8 K or better in the lower stratosphere while observed biases based upon comparisons with previously validated satellite-based measurements range from 0 to +1 K in the lower stratosphere.

To investigate the mechanisms behind the QBO signature on the AM water vapour, we used daily values of wind, temperature and fraction of cloud cover from the ERA5 reanalysis (Hersbach et al., 2020) over the period 2005-2020. The ERA5 reanalysis, based on the Integrated Forecasting System (IFS), has a horizontal resolution of 31km and 137 vertical levels that extend to 0.01 hPa. In this study, the fields of wind, temperature and fraction of cloud cover obtained from this reanalysis have been interpolated onto a 2.5º × 2.5º longitude and latitude grid, and they are extracted from the analysis available at 37 pressure levels between 1000hPa and 1hPa. Regarding the fraction of cloud cover, the comparison performed by Yao et al. (2020) between ERA5 and data from the Moderate Resolution Imaging Spectroradiometer (MODIS) aboard the Terra and Aqua satellites showed that differences of monthly mean cloud cover between ERA5 and MODIS are mostly around or less than 5% over the tropical and subtropical regions where, additionally, the correlation coefficients between these two datasets are larger than 0.8. These results allow us to conclude that the interannual variability of cloud cover is reasonably captured by ERA5.

https://doi.org/10.5194/egusphere-2023-1432
Preprint. Discussion started: 11 July 2023

Together with ERA5 fraction of cloud cover, NOAA-interpolated outgoing longwave radiation (OLR) data (Liebmann and Smith, 1996) is also used as a proxy for deep convection. We use the daily data interpolated onto a 2.5º × 2.5º longitude and latitude grid provided by the NOAA/OAR/ESRL PSL, Boulder, Colorado, USA, from their web site at *https://www.psl.noaa.gov/.*

In this study, Singapore sonde monthly zonal wind have been used to define the QBO phases at five pressure levels between 70hPa and 10hPa and for two different months separately, July and August. Each wind value corresponding to each month and level was standardized by subtracting the average value for the period of study, 2005-2020, and dividing by the standard deviation. Then, the QBO easterly (E-QBO) and westerly phase (W-QBO) at each level correspond to those cases in which the standardized zonal wind values were below -0.5 or above 0.5. Table 1 shows the number of W-QBO and E-QBO cases obtained for each month and pressure level.

	10hPa	**20hPa**	**30hPa**	**50hPa**	**70hPa**
July	7/6	8/6	8/7	8/6	5/5
August	7/6	9/6	9/7	9/5	7/5

Table 1: Number of cases of W-QBO/E-QBO cases obtained for July and August at each pressure level.

3 The QBO impact on the AM water vapour and the role of temperature

In order to assess the QBO impact on the lower stratosphere water vapour over the Asian Monsoon, we computed QBO-W minus QBO-E differences of MLS water vapour at 100hPa and 82hPa. Although, in principle, we considered all months in which the Asian Monsoon is active, from June to September, we only detected a significant QBO signal in July and August (Figs. 1 and 2 respectively). Therefore, we have excluded from our analysis the months of June and September, during which we did not find significant anomalies over the Asian Monsoon (not shown).

As expected, Figures 1 and 2 show a QBO modulation of the water vapour over equatorial latitudes, which is a well-known response to the QBO signature on equatorial temperatures. For the QBO defined at 10hPa water vapour decrease up to 0.7 ppmv over the tropics during both July and August while the signature weakens for the QBO phases defined at levels from 20hPa to 30hPa. Finally, when the QBO phases are defined at 50hPa, Figures 1 and 2 show a moistening of the tropics during W-QBO, consistent with anomalously warm tropical temperatures during westerly QBO phase. This moistening reaches around 0.7 ppmv for the QBO defined at 70hPa. The QBO impact on the tropical water vapour is also evident, although weaker, at 82hPa (Figs. 1 and 2, right column), which is consistent with the existence of a QBO tape recorder resulting from its modulation of the tropical cold point tropopause (Geller et al., 2002).

https://doi.org/10.5194/egusphere-2023-1432
Preprint. Discussion started: 11 July 2023

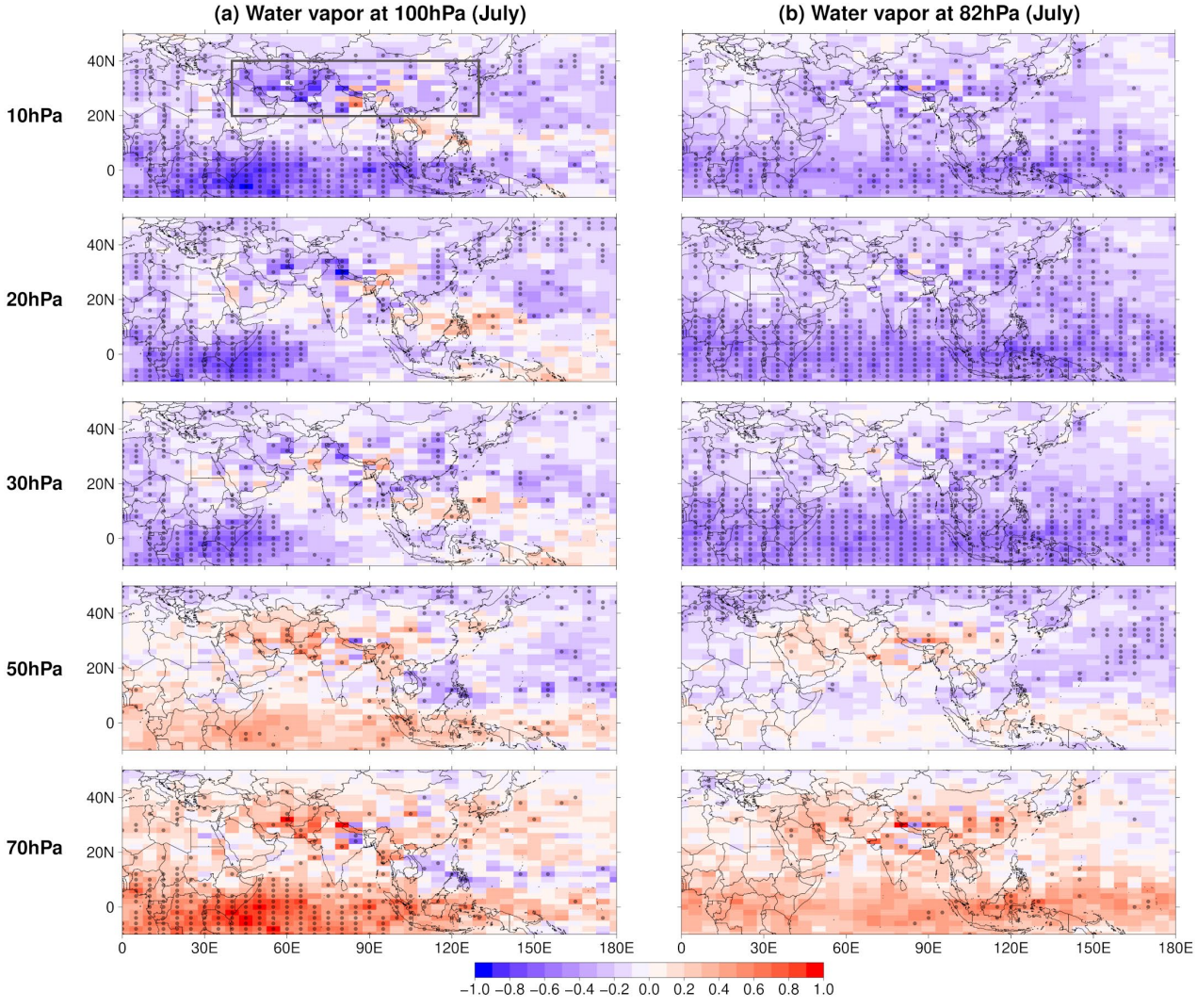

Figure 1: QBO-W minus QBO-E differences for MLS water vapour at 100hPa (a) and 82hPa (b) for July over the period 2005-2020. Each row corresponds to a different level at which the QBO phases were defined from 10hPa (top row) to 70hPa (bottom row). Dots indicate significance at the 95% confidence level. The region inside the grey box corresponds to the Asian monsoon region during the QBO phase in which we have identified a stronger signal on the water vapour of this area.

https://doi.org/10.5194/egusphere-2023-1432
Preprint. Discussion started: 11 July 2023

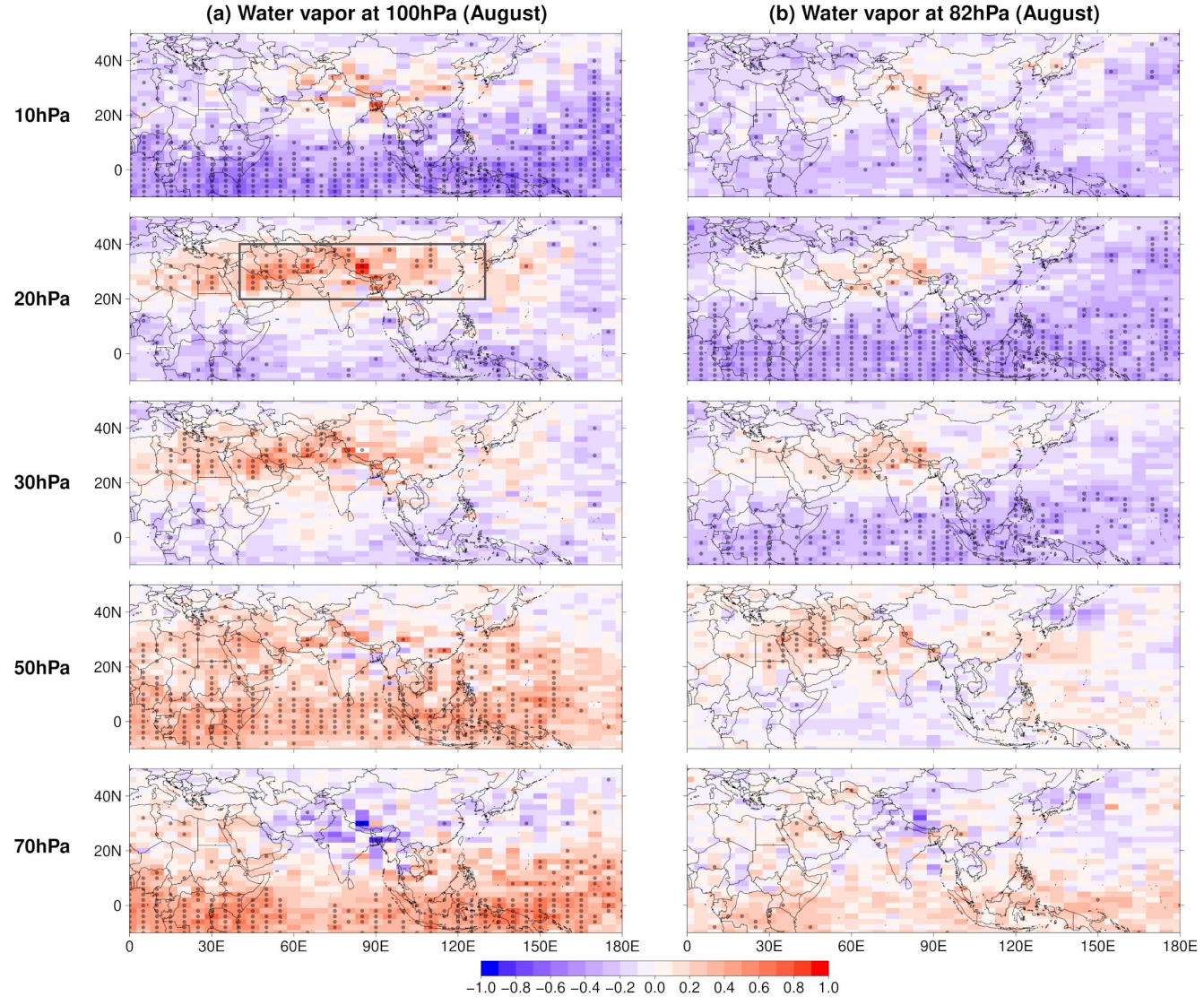

Figure 2: QBO-W minus QBO-E differences for MLS water vapour at 100hPa (a) and 82hPa (b) for August over the period 2005-2020. Each row corresponds to a different level at which the QBO phases were defined from 10hPa (top row) to 70hPa (bottom row). Dots indicate significance at the 95% confidence level. The region inside the grey box corresponds to the Asian monsoon region during the QBO phase in which we have identified a stronger signal on the water vapour of this area.

By contrast with the signal on the tropical water vapour, the QBO signals over the AM shows an opposite behaviour in July and August. Thus, while during July the QBO signal over the AM and the tropics are in phase, they show opposite signs during August. As established in previous studies, the UTLS temperature plays a key role in the control of water vapour over the AM (Wright et al., 2011 and Randel et al., 2015). Furthermore, Randel et al. (2015) found that, at intraseasonal time scales, there is a lag between temperature and its impact on the AM water vapour of around 10 days. Therefore, in order to assess the link

https://doi.org/10.5194/egusphere-2023-1432
Preprint. Discussion started: 11 July 2023

between the QBO impact on temperature and on water vapour, we first identify those regions whose temperature exerts the greatest control over the AM water vapour and the lag that characterises this link. To identify these regions we computed running correlations between the AM water vapour and the 100hPa temperature field at each grid point. For that purpose, we calculated the regional average of water vapour over the AM domain (20ºN–40°N and 40ºE–140°E) for July and August over the period 2005-2020 and the averages of the daily temperatures over 31-day running windows from June 1st to September 30th at each grid point over the same time period. Results for July show maximum correlations for the temperature over the tropical Indian Ocean average between 16 June and 16 July (Figs. 3a). For this period of the year, significant correlations extend from the tropical Indian Ocean to southern India reaching values up to 0.8 over some regions of the Indian Ocean. For the temperature average over this region, correlations with the AM water vapour for July achieve a maximum value of 0.8 that slowly decreases as the time window moves away from the maximum correlation period, 16 June - 16 July (Fig. 3b, dark blue line). This result indicates that the temperature over the Indian Ocean is key in the control of the interannual variability of the AM water vapour during July and that its impact peaks with a time lag of about 15 days between the temperature signal and the water vapour response. It is not only in the tropical Indian Ocean that significant correlations are found. Positive correlations extend zonally over the equatorial region (not entirely shown in Fig. 3a) forming a spatial pattern consistent with the QBO signal on temperature in the tropics. By contrast, results for August show maximum correlations over India, which peak for the temperature field averaged between 19 July and 18 August (Figs. 3c and 3d), implying that there is a time lag of about 12 days between the temperature signal and the water vapour response. Furthermore, contrary to what was found for July, the AM water vapour content during August is not significatively correlated with equatorial temperatures (Fig. 3c).

In spite of the fact that different climate patterns may contribute to the interannual variability of the AM water vapour in the lower stratosphere (e.g., ENSO), the QBO is expected to be a major source of variability at this timescale. Thus, we make use of the spatial and temporal features of the connection between temperature and AM water vapour observed in Fig. 3 to assess the link between the QBO impact on temperature and water vapour.With this aim, Figure 4 represents QBO related differences for the temperature at 100hPa averaged over those time windows that maximise the impact on the interannual variability of the AM water vapour during July (16 June - 16 July) and August (19 July - 18 August). For the average over the period 16 June – 16 July, QBO westerlies at 10 hPa and 20 hPa are linked to negative temperature anomalies, when compared with the QBO easterly phase, at the equatorial UTLS (Fig. 4a) and over the tropical Indian Ocean, which is the region controlling the water vapour over the AM during this month (Fig. 3a). This cooling is consistent with the anomalously dry stratosphere found in July over both the tropics and the AM in Fig. 1. On the contrary, water vapour increases are found in both regions for QBO westerlies defined at 50hPa and 70hPa (Fig. 1), following the temperature increase observed at the equatorial UTLS during the previous weeks (Fig. 4a). During this time, QBO related differences reach their maximum for the QBO phase defined at 10hPa, when temperature differences over the Indian Ocean between -1 K and -2 K precede a water vapour decrease of around -0.4 ppmv that can reach -0.8 ppmv to the western India. Hence, this relation between stratospheric water vapour and temperature in the monsoon region is consistent with the expected about 0.5ppmv entry water vapour change for a 1K temperature change for globally averaged inter-annual anomalies, as found by Fueglistaler and Haynes (2005).

https://doi.org/10.5194/egusphere-2023-1432
Preprint. Discussion started: 11 July 2023

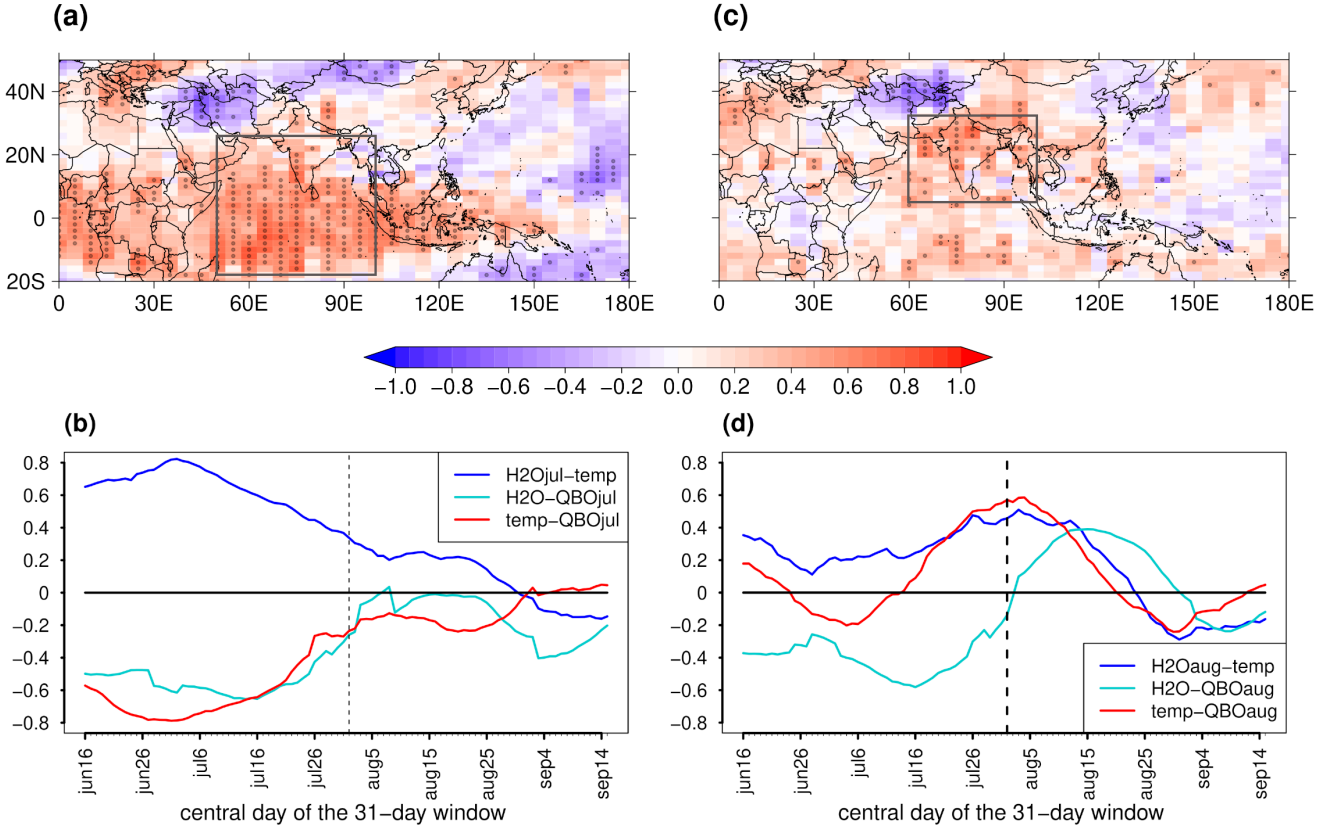

Figure 3: (a) Correlation between July water vapor at 100hPa over the AM [20N-40N, 40E-140E] and temperature at 100hPa at each grid point averaged between June 16th to and July 16th over the period 2005-2020.(b) Lag sliding correlations between July AM water vapor at 100hPa and temperaure averaged over the marked region in figure (a) [18S-26N, 50E-100E] and over 31-day running windows from June 1st to September 30th (dark blue line). Light blue and red lines represent lag sliding correlations between the QBO index for July at 10hPa and the AM water vapor (light blue line) and temperature (red line) averaged over the marked region in figure (a), both variables averaged over 31-day running windows from June 1st to September 30th. (c) Correlation between August water vapor at 100hPa over the AM [20N-40N, 40E-140E] and temperature at 100hPa at each grid point averaged between July 19th to and August 18th over the period 2005-2020. (d) Lag sliding correlations between August AM water vapor at 100hPa and temperaure averaged over the marked region in figure (c) [5N-35N, 60E-100E] and over 31-day running windows from June 1st to September 30th. Light blue and red lines represent lag sliding correlations between the QBO index for August at 20hPa and the AM water vapor (light blue line) and temperature(red line) averaged over the marked region in figure (c), both variables averaged over 31-day running windows from June 1st to September 30th.

https://doi.org/10.5194/egusphere-2023-1432
Preprint. Discussion started: 11 July 2023

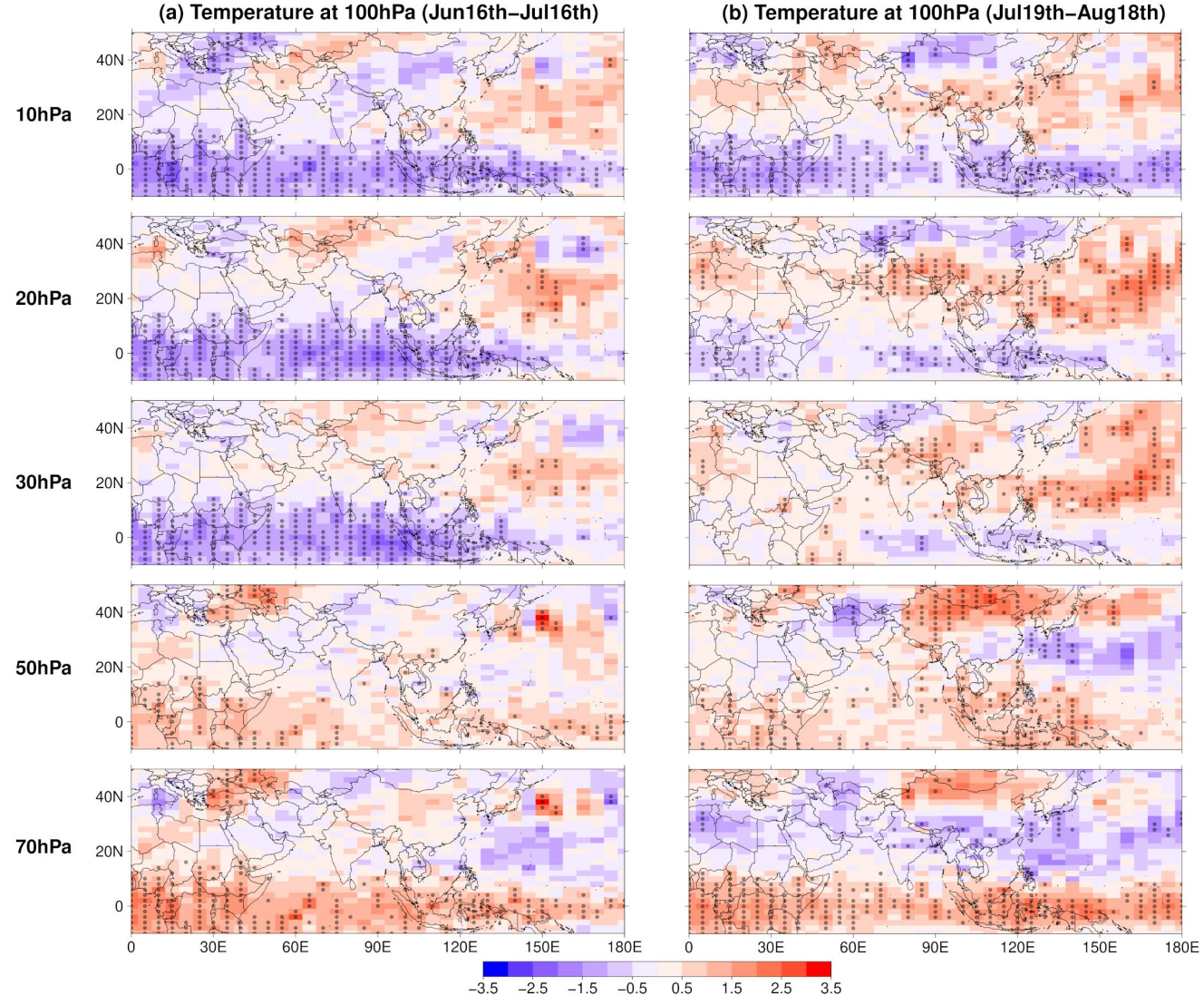

Figure 4: QBO-W minus QBO-E differences for MLS temperature at 100hPa averaged over the 31-day period between 16 June and 16 July (a) and between 19 July and 18 August (b), over 2005-2020. Each row corresponds to a different level at which the QBO phases were defined from 10hPa (top row) to 70hPa (bottom row). Dots indicate significance at the 95% confidence level.

So far, we have found a significant QBO signature on the temperature of the tropical Indian Ocean for the 16 Jun – 16 Jul time window, which is consistent with the AM water vapour response in July. However, in order to establish a causal link between water vapour and temperature it is important to see whether they have a consistent temporal behaviour. Figure 3b represents the cross-correlation between the QBO index for July at 10hPa and AM water vapour (light blue line) and average Indian Ocean temperature (red line). Running windows of 31 days from 1 June to 30 September have been used to calculate the lagged correlations. We chose 10hPa for the definition of the QBO index for July since it is for this level that the QBO impact on

https://doi.org/10.5194/egusphere-2023-1432
Preprint. Discussion started: 11 July 2023

water vapour is the strongest for this month (Fig. 1). These results evidence that while correlations reach a maximum centred in the month of July for water vapour (Fig. 3b, light blue line), the QBO impact on the tropical Indian temperature peaks around 15 days before (Fig. 3b, red line), which is consistent with the lag found between temperature and the interannual variability of the AM water vapour during July (Fig. 3b, dark blue line).

In contrast to what is observed for July, during August Fig. 2 reveals significant water vapour anomalies over the Asian Monsoon that are of opposite sign with respect to those over the equator. This is consistent with the QBO signal on the average temperature for the period 19 July-18 August shown in Fig. 4b, which shows a branch of significant temperature anomalies at subtropical latitudes with opposite sign compared to equatorial regions. These subtropical temperature anomalies extend over India, the region whose temperature, as shown in Fig. 3c, has a major impact on the interannual variability of the AM water vapour during August. In fact, the comparison of Figs. 2 and 4b evidences that the sign and magnitude of the temperature anomalies observed for each QBO phase over this key region is in agreement with the QBO signature on water vapour over the AM. Thus, for the QBO phase defined at 20hPa both AM water vapour and temperature anomalies over northern India and southwestern China reach their maximum, with values between 0.3 ppmv and 1 ppmv and 0.5 K and 1 K respectively. For the QBO defined at 50hPa, temperature and AM water vapour anomalies weaken, while a slight drying of the AM is observed at the same time as temperature decreases over northern India and southwestern China when QBO westerlies prevail at 70hPa.

Figure 3d allows us to analyze the temporal evolution of the impact of the QBO on water vapour in the Asian Monsoon in August and on the temperature over India, which we have identified as the region that controls the interannual variability of water vapour over the Asian Monsoon (Fig. 3c). This figure represents the cross-correlation of the QBO index for August at 20hPa, the level for which the water vapour response reaches a maximum (Fig. 2), with the AM water vapour (Fig. 3d, light blue line) and the temperature over India (Fig. 3d, red line), both averaged over 31-day running windows from June 1st to September 30th. It confirms that indeed the QBO signal on temperature over India peaks during the 19 July - 18 August time window (the 31-day window centred around the 3rd-4th of August), with a lag of twelve days over the maximum in the QBO signal on the AM water vapour.

In order to explore further details of the three dimensional QBO temperature and wind patterns linked to the AM water vapour signature, Figure 5 shows the latitude-height cross sections of QBO-W minus QBO-E differences for temperature and zonal wind averaged over 60E-120E. After checking that ERA-5 reanalysis data reproduced the QBO signal on the temperature field at 100hPa (not shown), we used this dataset for the analysis of the three-dimensional temperature and wind variations over the AM associated with the QBO signature on the AM water vapour. In order to obtain the QBO anomaly pattern with the greatest impact on AM water vapour Fig. 5a shows QBO related differences for the QBO phases defined according to the equatorial zonal wind of July at 10hPa and for the time window between 16 Jun and 16 Jul while, for August Fig. 5b depicts differences for the QBO phases defined according to the August wind at 20hPa and for the time window between 19 Jul and 18 Aug.

https://doi.org/10.5194/egusphere-2023-1432
Preprint. Discussion started: 11 July 2023

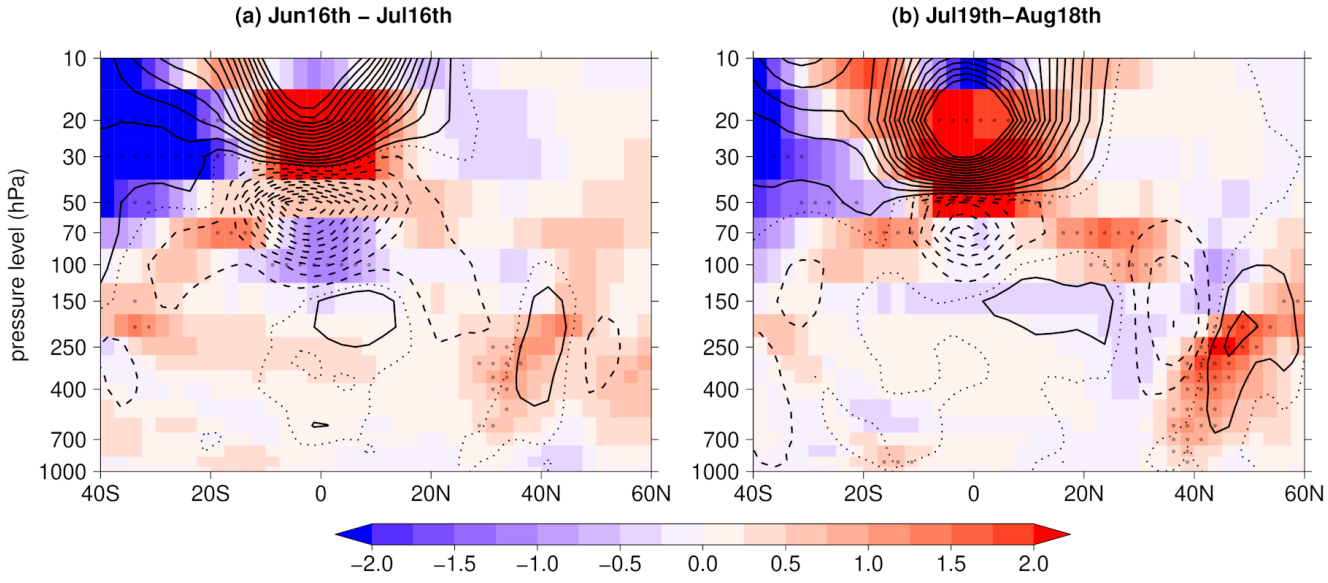

Figure 5: Latitude-height cross sections of QBO-W minus QBO-E differences for ERA5 temperature (colors) and zonal wind (black contours) averaged over 60E-120E and and between June 16th and July 16th (a) and between July 19th and August 18th (b). In (a) diifferences correspond to the QBO index for July defined at 10hPa while for (b) we chose the QBO index defined at 20hPa for August. Solid/dashed contour lines show positive/negative anomalies with contour intervals at every 2m/s from 1m/s/-1m/s for positive/negative anomalies. Dots indicate significance at the 95% confidence level.

In agreement with the chosen QBO phase definition, Figure 5 shows westerly wind anomalies at the upper stratosphere and easterly anomalies centered at 70hPa. The QBO also exhibits a signature in temperature in both tropics and subtropics. The tropical QBO temperature is in thermal wind balance with the vertical shear of the zonal winds and, according to this, Figures 5a and 5b show cold temperature anomalies in regions of the tropical UTLS with negative vertical shear. As it has been established in previous studies (Baldwin et al., 2001), besides the equatorial maximum in QBO temperature, out of phase anomalies may appear over 20º-40ºN associated to the secondary meridional circulation. Despite the fact that these subtropical anomalies are weaker in the summer hemisphere, the global zonal average for 16 June - 16 July shows warm anomalies in the region of the UTLS at these latitudes (Fig. A1a). However, these anomalies are not found over the southern flank of the AM (Fig. 5a), where only weak cold anomalies are found at 100hPa surrounded at upper and lower levels by weak warm anomalies that, in either case, are not statistically significant. By contrast, during August Fig. 4 already showed that for the QBO defined at 20hPa, the impact on subtropical temperatures at 100hPa is relatively strong over the southern flank of the Asian Monsoon. This is also evident when we compare the vertical profile of temperature anomalies averaged over 60E-120E (Fig. 5b) with those corresponding to the global average (Fig. A1b), which shows weaker anomalies over the northern subtropical region at 100hPa. Furthermore, Fig. 5b evidences that subtropical temperature anomalies over the longitude range corresponding to the AM extend over 20N-40N and from 100hPa to 50hPa and shows that they form part of a quadrupole structure characterized,

https://doi.org/10.5194/egusphere-2023-1432
Preprint. Discussion started: 11 July 2023

in the lower stratosphere, by positive and negative anomalies in the southern and northern flanks of the AM and out of phase anomalies in the troposphere. Fig. 5b also shows consistent variations of the zonal wind in thermal wind balance with the temperatures in a way that wet anomalies (as evident from Fig. 2) are linked to a weaker anticyclone, a cold troposphere and warm lower stratosphere in the latitude range between 25-35ºN and temperature anomalies of opposite sign north of 35ºN. This is consistent with Randel et al. (2015), who found that the intraseasonal variability of the AM water vapour was linked to a similar pattern of temperature and zonal wind anomalies.

So far, our results demonstrate that the QBO modulation of the LS temperatures over certain key regions precede consistent water vapour variations over the AM. These temperature variations, in turn, provoke a QBO signature on the AM water vapour that is in phase with the signature over the equatorial and tropical region during July and out of phase during August.

4 The role of the QBO modulation of deep convection

Previous studies have found that the QBO modulates deep convection over the AM (Giorgetta and Bengtsson, 1999; Peña-Ortiz et al., 2019). In addition, Randel et al. (2015) showed evidence that temperature variations that precede the intraseasonal changes in AM water vapour are linked to convection changes. In this way, they found that enhanced convection over the southeastern AM produced a colder UTLS over this region, giving rise to drier conditions over the AM. These results raise the question of whether a similar mechanism operates on an interannual scale and, more specifically, whether convection plays a role in the transmission of the QBO signal to AM water vapour. To address this question, we have made use of OLR and fraction of cloud cover as a proxy for convection and have computed QBO-W minus QBO-E differences for the same time windows as used for the temperature. Thus, differences were computed for the averages between 16 Jun and 16 Jul for the analysis of the QBO signal on water vapour in July and for the average between 19 Jul and Aug18th for August. Additionally, the chosen level for the definition of the QBO phases used for each case corresponds with the one that maximizes the QBO signature on water vapour during July and August, which are 10hPa and 20hPa respectively.

Figures 6a and 6b show QBO-W minus QBO-E (defined at 10hPa) differences for fraction of cloud cover averaged between 16 Jun and 16 Jul at 100hPa and also for the average between 125hPa and 150hPa. These levels were chosen after verifying that the QBO signal on cloudiness significantly weakens below 150hPa (Fig. 6d), which is consistent with previous studies (Giorgetta et al., 1999; Peña-Ortiz et al., 2019). Figure 6b shows positive anomalies of fraction of cloud cover between 125hPa and 150hPa over the equatorial Indian Ocean and Indonesia that indicate a convection increase during the westerly phase of the QBO (as defined at 10hPa, corresponding to an easterly phase around 100-70hPa, see Fig. 5) that can reach about 10% over some areas. A similar behaviour is found at 100hPa (Fig. 6a), although anomalies are weaker at this level. Consistently, OLR anomalies show negative values over this region during the QBO-W (Fig. A2a). These results are in agreement with previous studies (Giorgetta et al., 1999; Collimore et al., 2003; Peña-Ortiz et al., 2019) evidencing that the temperature anomaly initiated by the adiabatic temperature change due to the secondary circulation of the QBO can modulate deep convection in a

https://doi.org/10.5194/egusphere-2023-1432
Preprint. Discussion started: 11 July 2023

way that the UTLS cooling linked to the easterly QBO jet at lower levels around 100-70hPa causes a lower static stability that allows deep convection to develop more vigorously.

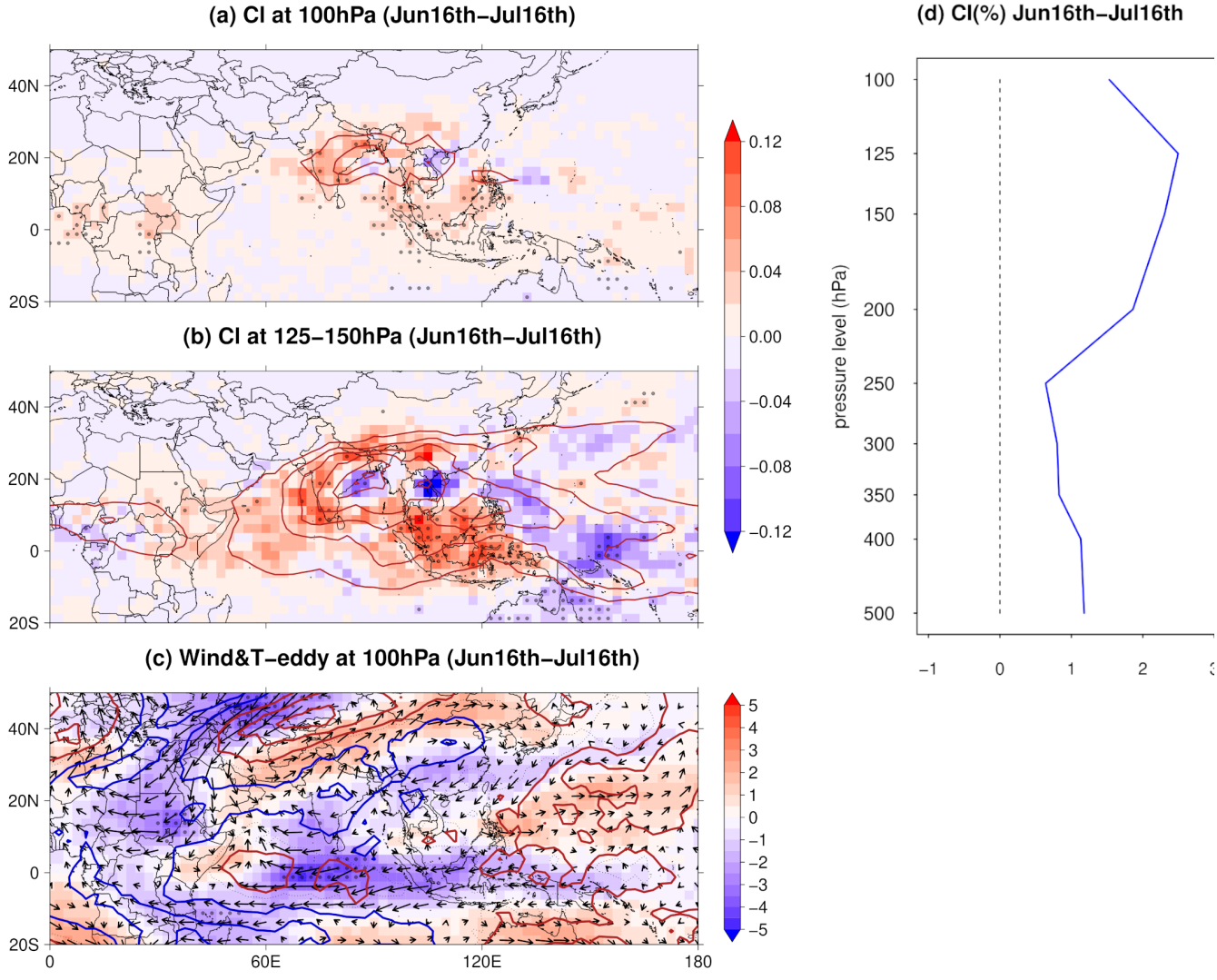

Figure 6: QBO-W minus QBO-E differences for the average over the period 16 Jun – 16 Jul of fraction of cloud cover at 100hPa (a) and for its average between 125hPa and 150hPa (b). Red solid lines represent the climatological average for the same time window and over the period 2005-2020. (c) Equivalent differences for eddy fields of zonal wind (color shades) and horizontal wind (arrows). Blue/red contour lines show negative/positive anomalies of the temperature eddy field with contour intervals at every 0.5K starting at 0.25K and -0.25K for positive and negative anomalies respectively. (d) Similar differences but for fraction of cloud cover averaged over 60E-120E and 15S-25N, the region with the largest anomalies, at different pressure levels from 500hPa to 100hPa. Dots indicate significance at the 95% confidence level.

https://doi.org/10.5194/egusphere-2023-1432
Preprint. Discussion started: 11 July 2023

However, the impact of the QBO on convection is not limited to the equatorial Indian Ocean, where temperature variations associated with the secondary circulation of the QBO can explain this signal. Beyond the equator, a significant increase in cloud cover during the westerly phase of the QBO (defined at 10hPa) is also observed over India (Figs. 6a and 6b). This cloud cover change suggests an increase in the convective area while less intensity in the core region, as main positive changes are around the core region of climatological convection. The increase in cloud cover is associated with an intensification of the anticyclonic circulation over this area, as seen in Fig. 6c showing the 100hPa zonal wind eddy field. Our results suggest that the anticyclonic anomaly and the convection increase over India can be part of the response to the enhanced convection over the Equator. Previous studies (Matsuno 1966; Gill 1980; Dima et al. 2005) have established that the tropical response to deep convection is characterized by a Matsuno–Gill-type Rossby–Kelvin wave couplet pattern. The Matsuno–Gill model explains that zonally varying tropical heating, which could be caused by deep convection, gives rise to Kelvin and Rossby waves extending eastward and westward, respectively, of the region of heating. Rossby waves, in turn, can propagate poleward (visualized by ‘‘wavetrains’’) and around the globe. This is observed in Fig. 6c which evidences that, at 100 hPa, the diabatic heating linked to the cloud formation produces the divergence of the eddy anomalies of the zonal wind out of the region of convection. Consequently, an easterly wind anomaly is found at, and to the west of, the heating region, giving rise to two anticyclonic gyres at about 20°N, over India, and at 10ºS (Fig. 6c). Thus, the northern anticyclone would be part of the Rossby wave trains generated by the QBO modulation of convection over the equator, contributing to the strengthening of the climatological AM anticyclonic circulation and giving rise to an enhancement of the rising motions and deep convection.

Previous studies (Muhsim et al., 2018; Johnston et al. 2018) have pointed out that deep convection causes a cooling of the tropical tropopause layer (TTL) just below the cold point tropopause (CPT), due to adiabatic upwelling and longwave cooling. Consistently, Figure 6c, which depicts the temperature eddy field at 100hPa, shows that the increased cloudiness in the UTLS causes a cooling over India of up to 1 K, which is slightly higher than the cooling observed when we consider the total temperature field in Fig. 3 (wavefield plus zonal average). The reason for this difference is the zonal mean temperature, which shows a warming associated with the secondary circulation of the QBO over subtropical latitudes (Fig. A1a). Thus, these results suggest that the modulation by the QBO of the convection over the equator during the month of July causes a wave train that intensifies the convection over India resulting in the observed cooling over this region. This subtropical cooling occurs simultaneously with the equatorial cooling associated with the secondary circulation of the QBO, such that, the entire region whose temperature modulates the transport of water vapour in the AM, shows a cooling during the westerly phase of the QBO (as determined by the 10 hPa tropical zonal wind). This explains why the signal on water vapour in the AM has the same sign and characteristics as the signal on equatorial water vapour and why in both regions a decrease in its concentration is observed during QBO-W in relation to QBO-E.

Concerning the QBO modulation of the AM water vapour during August, QBO-W minus QBO-E (defined at 20hPa) differences for the average between 19 Jul and 18 Aug of cloud area fraction (Figs. 7a and 7b) reveal a quite different behaviour with respect to the anomalies for 16 June – 16 July (Figs. 6a and 6b). A northward and westward shift of the anomalies is observed during 19 Jul – 18 Aug, suggesting that the impact of the QBO on convection weakens over the equator

https://doi.org/10.5194/egusphere-2023-1432
Preprint. Discussion started: 11 July 2023

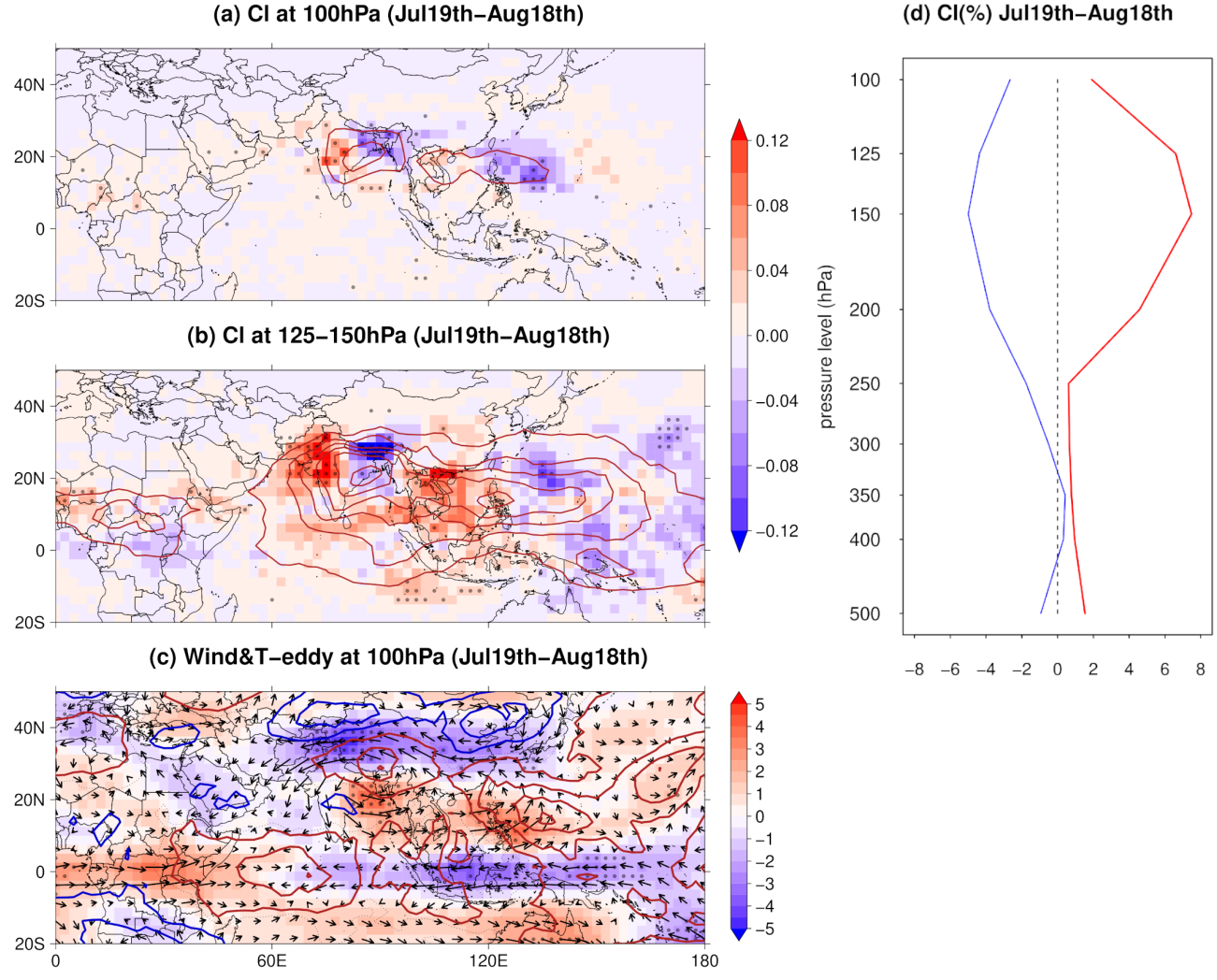

Figure 7: QBO-W minus QBO-E differences for the average over the period 19 Jul – 18 Aug of fraction of cloud cover at 100hPa (a) and for its average between 125hPa and 150hPa (b). Red solid lines represent the climatological average for the same time window and over the period 2005-2020. (c) Equivalent differences for eddy fields of zonal wind (color shades)and horizontal wind (arrows). Blue/red contour lines show negative/positive anomalies of the temperature eddy field with contour intervals at every 0.5K starting at 0.25K and -0.25K for positive and negative anomalies respectively. (d) Similar differences but for fraction of cloud cover averaged over 60E-80E and 20N-30N (red line) and over 80E-95E and 20N-30N (blue line), regions with the largest anomalies, at different pressure levels from 500hPa to 100hPa. Dots indicate significance at the 95% confidence level.

and intensifies at latitudes higher than 15N as the boreal summer progresses. Figures 7a and 7b evidence a dipole structure characterized by a decrease/increase of convection over the southeastern/southwestern flank of the AM during QBO-W compared to QBO-E. A consistent pattern is found for OLR anomalies (Fig. A2b). Figure 7d shows that, as for June/July (Fig.

https://doi.org/10.5194/egusphere-2023-1432
Preprint. Discussion started: 11 July 2023

6d), cloud area fraction anomalies are restricted to the atmospheric layer between 200-100hPa. The weakening of convection observed in Figs. 7a and 7b is linked to a cyclonic anomaly (Fig. 7c) and occurs over the area of the climatological maximun in August. To the west of this area, positive anomalies of cloud area fraction indicate an enhancement of convection, evidencing a westward shift of the convective activity during QBO-W in comparison with QBO-E.

Figure 7c reveals that the weakening of convection observed over the southeastern AM during QBO-W is linked to a Rossby wave train that generates the cyclonic gyre over this region. The QBO signature on the zonal wind eddy field reveals a Rossby wave train that propagates from the equator to extratropical latitudes over both hemispheres between the eastern Indian and the western Pacific oceans. This figure, that also shows QBO related differences in the eddy temperature field, evidences that the weakening of convection over the region of the climatological maximum gives rise to a warming over the southern flank of the AM that, as previously shown, controls the inflow of water vapour into the AM. On the other hand, QBO-W minus QBO-E differences of the global zonal mean temperature averaged over the period 19 Jul and 18 Aug (Fig. A1b) shows a warming in the lower stratosphere between 15N and 35N, corresponding to the subtropical branch of the secondary circulation of the QBO. Thus, during this time window, the real temperature field over the southern flank of the AM reflects a temperature increase for the QBO westerly phase defined at 20hPa (Fig. 4b, second row), which is caused by both a Rossby wave train associated to the QBO that weakens convection over this region and the secondary meridional circulation of the QBO. Therefore, both mechanisms contribute to the warming that gives rise to the water vapour increase found during August over the AM.

Giorgetta et al. (1999) found that the QBO modulation of deep convection over the AM gives rise to the excitation of a wave train. They observed that despite the fact that this wave train reached its mature phase in July/August, it was forced by equatorial diabatic heat release in the previous weeks by the QBO modulation of equatorial deep convection. In order to study the possible link between convection and the wave train observed in Fig. 7c, we computed QBO-W minus QBO-E composites for cloud cover and the eddy field of horizontal wind for different 31-day windows prior to the one between 19 Jul - 18 Aug, using always the QBO index defined for August at 20hPa. In this way, we can observe the QBO modulation of convection and the eddy fields in the weeks preceding the formation of the wave train observed in Fig. 7c. The obtained results are shown in Fig. 8, which depicts these differences for the time windows between 1 Jul – 31 Jul, 10 Jul – 9 Aug and 19 Jul - 18 Aug. This figure reveals that in the preceding weeks, the QBO modulation of convection gives rise to a dipole structure characterized by a strengthening over the eastern Indian Ocean, India and Indonesia and a weakening over the Western Pacific Ocean (Fig. 8a). The dynamical response to these anomalies is shown in Fig. 8b, that depicts a pattern consistent with the Matsuno–Gill model. The eddy anomalies of the zonal wind diverge from the region of positive cloud cover anomalies due to the release of diabatic heating associated with the enhancement of convection. Thus, an easterly wind anomaly is found over the equatorial Indian Ocean, associated to the enhancement of convection, and a westerly wind anomaly over the western Pacific. The westerly wind anomaly developed to the east of Philippines is linked to a cyclonic gyre centred around 25N. If we observe the evolution of these patterns in the following days, it is found that as positive convective anomalies weaken over the tropics, the easterly wind over the Indian Ocean also weakens while the cyclonic gyre previously mentioned extends westward over southern China

https://doi.org/10.5194/egusphere-2023-1432
Preprint. Discussion started: 11 July 2023

and northern India (Figs. 8c and 8d). In the following days (Figs. 8e and 8f) this cyclonic anomaly strengthens over the Bay of Bengal while an anticyclone developes to the north of it forming the Rossby wave train observed in Fig. 7d for the time window 19 Jul-18 Aug.

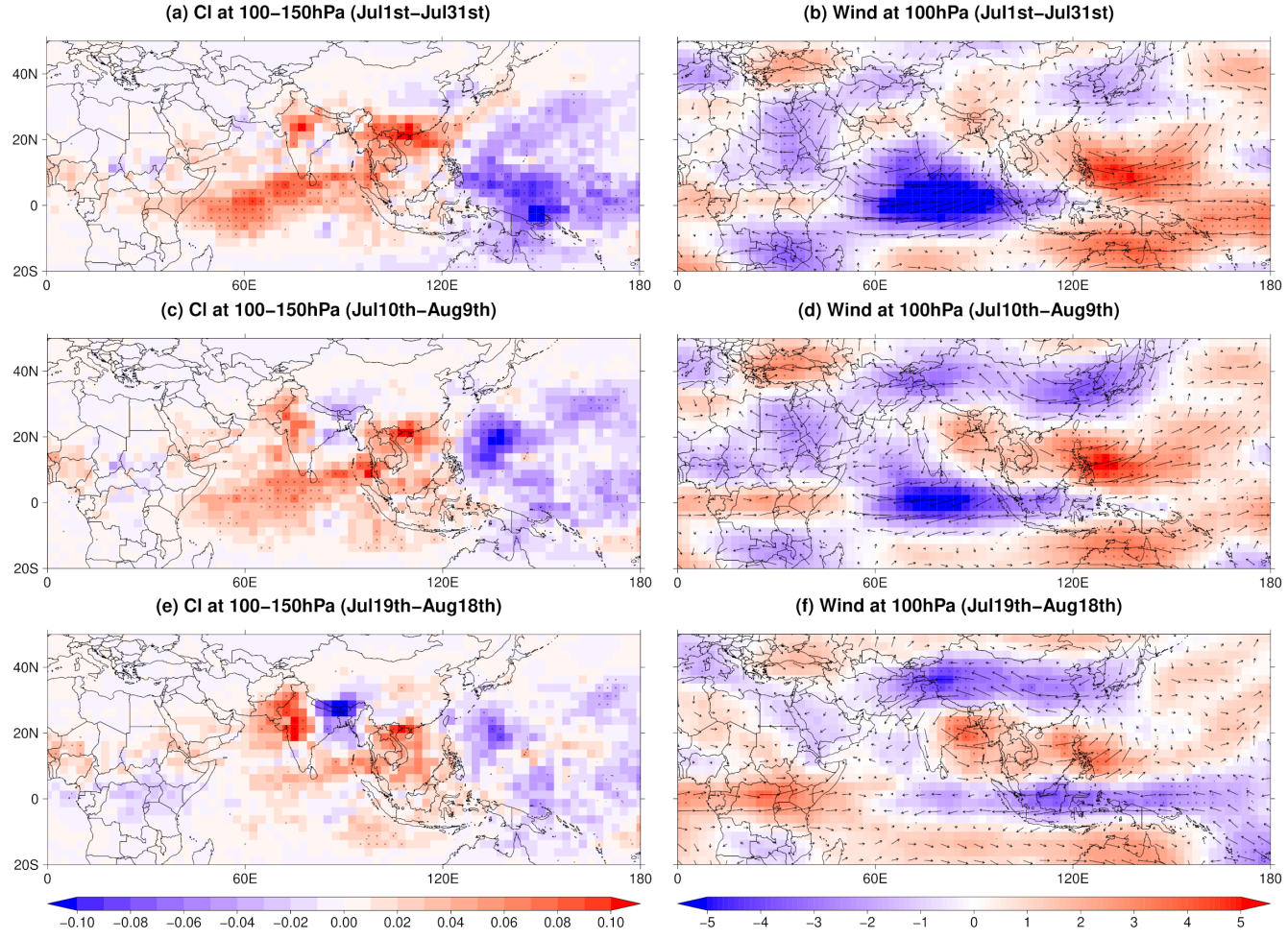

Figure 8: QBO-W minus QBO-E differences for cloud fraction (color shades) at 100hPa (a) and for the eddy fields of zonal wind (color shades) and horizontal wind (arrows) (b) averaged over the period between 1st July and 31st July. (c)-(d) and (e)-(d) are equivalent to (a)-(b) but for the periods 10th July- 9th August and 19th July- 18th August respectively. Dots indicate significance at the 95% confidence level.

5 Conclusions and discussion

The Asian Monsoon plays a key role in the transport of water vapour to the lower stratosphere and contributes significantly to the wet phase of the annual global stratospheric water vapour cycle. The interannual variability of the lower stratospheric

https://doi.org/10.5194/egusphere-2023-1432
Preprint. Discussion started: 11 July 2023

water vapour over the Asian Monsoon is dominated by the QBO and ENSO (Randel et al., 2015). However, the physical mechanisms responsible for this variability have been poorly investigated.

Here we have made use of daily MLS data for the period 2005-2020 to characterize the QBO signature on the lower stratosphere AM water vapour during the boreal summer. We have found that the QBO has the strongest impact during August, although a significant signature is also observed during July. In July, the QBO modulation of the AM water vapour occurs in phase with the modulation of the lower stratospheric water vapour over the equator. Hence, as the equatorial UTLS cools as a response to the QBO winds, the water vapour over the tropical lower stratosphere and the AM decreases and vice-versa. This synchrony is related to the fact that, in this month, the region whose temperature controls the water vapour variability associated with the QBO over the AM is the UTLS over the tropical Indian Ocean, which also modulates the inflow of water vapour across the equator over this region. Although the south side of the AM anticyclone is a key region in controlling water vapour over the Asian monsoon (Wright et al., 2011; Randel et al., 2015), we find that in July the QBO signal on temperature is weak over this region and only significant over western India and the Arabian Sea, which shows anomalies of the same sign as the signal over the equator. These results suggest that the AM water vapour signal in July responds to the QBO temperature over a large region stretching from the tropical Indian Ocean to the northern Arabian Sea and western India, where the QBO signal on temperature is in phase. Furthermore, our results show a time lag between the temperature and water vapour signal over the AM of about 15 days. In this way, temperature anomalies over the tropical Indian Ocean of -1 K and -2 K precede a water vapour decrease of around -0.4 ppmv that can reach -0.8 ppmv to the west of India.

Conversely, in August the region whose temperature controls water vapour inflow to the AM is primarily the northern Bay of Bengal, northwestern India and southeastern China. This is consistent with Randel et al. (2015), who pointed to the temperature over this region as the main driver of the intraseasonal variability of AM water vapour. Moreover, by contrast with the QBO signal on temperature in July, during August, the UTLS over this region shows temperature anomalies associated with the QBO of opposite sign to those over the equator and, for this reason, the QBO signal on the lower stratospheric water vapour over the equator shows an opposite sign to the signal over the AM. In August, the QBO signature on the AM water vapour reaches its maximum when we define the QBO phase at 20hPa. Then we observe that, with a time lag of about 12 days, the signal in the temperature of this region shows a warming during the QBO westerly phase compared to the easterly phase of 0.5 K to 1 K ,which causes an increase in humidity over the monsoon of between 0.3 and 1 ppmv.

Regarding the mechanism involved in the observed patterns, our results reveal that the QBO impact on the temperature at the southern flank of the AM and, consequently, on the AM water vapour during July and August, is modulated by the QBO impact on convection. For the QBO signatre on the AM water vapour during July, our results show that QBO cold anomalies over the equator intensify convection over the eastern Indian Ocean and Indonesia during the preceeding weeks, as can be observed by an increase in cloud cover at levels between 150hPa and 100hPa. Eddy temperature and wind fields show a response to these convection anomalies that produces a Rossby anticyclonic gyre at 100hPa over India, which intensifies convection, giving rise to a cooling over this region. This cooling, which is clearly observed in the eddy temperature field, is partially balanced by the zonal mean temperature, which shows a warming associated with the secondary circulation of the

https://doi.org/10.5194/egusphere-2023-1432
Preprint. Discussion started: 11 July 2023

QBO over subtropical latitudes. As a result, the total temperature field over the southern flank of the AM shows a slight and not significant cooling during QBO-W (defined at 10hPa). This absence of a strong QBO impact on subtropical temperatures over the southern flank of the AM, explains the reason why during July the QBO signature on the AM water vapour is modulated by QBO temperature anomalies over the equator and the fact that the QBO modulation of AM water vapour is in phase with its modulation of the lower stratosphere water vapour over the equatorial region.

Our results also evidence a relationship between the QBO modulation of the AM water vapour during August and convection. Temperature anomalies over India, preceding the QBO-associated changes in AM water vapour, are consistent with the observed changes in convection. In this way, the observed warming over the region that controls the inflow of water vapour into the monsoon, north of the Bay of Bengal, is accompanied by a decrease in cloud cover in the 100-150hPa layer over this same region, which in turn is the region of the climatological maximum of convection. At the same time, an increase in cloud cover is observed to the west of this region, over northwest India, although this increase is relatively weak at 100hPa and stronger between 125 and 150hPa. These results reveal that water vapour changes over the Asian Monsoon are associated with a westward shift of convection, characterized by anomalously strong convection in the southwest and weak convection in the southeast of the AM. Remarkably, previous studies (Randel et al., 2015; Zhang et al., 2016) found a dipole pattern in intraseasonal convective variability very similar to the pattern found here for QBO-related variability, with similar effects on the AM water vapour. In this regard, Randel et al. (2015) pointed out the apparent contradiction arising from the fact that a reduction of convection over the region of the climatological maximum is associated with an increase, rather than a reduction, of humidity over the AM. Hence, this study demonstrates that the intra-seasonal water vapour variability in the AM is related to the upper-level temperature response to convective variability in that region (i.e. cooling/warming due to enhanced/weakened convection), which is key in the dehydration of the air parcels reaching the AM. A similar response is clearly observed in our results which show a warm anomaly over the region where the reduction in cloud cover appears. Furthermore, Zhang et al. (2016) found that, at intraseasonal time scales, the intensification of convection over the west pole implies an increase in upward motions over this region, which is warmer than the southeast flank of the AM. They showed that this westward shift of the AM convective systems favours the entry of air masses into the AM through this region, allowing them to transport a higher water vapour amount. Our results suggest that a similar mechanism also contributes to the QBO impact on the AM water vapour during August.

The modulation of convection over the southeastern flank of the AM is linked to a Rossby wave train associated with the QBO that propagates from the equator to extratropical latitudes over both hemispheres between the eastern Indian and the western Pacific oceans. Thus, the weakening of convection found over the region of the climatological maximum when QBO westerlies dominate at 20hPa, is linked to a cyclonic gyre over this region that forms part of the wave train, as it can be observed in the eddy wind field at 100hPa. Furthermore, in agreement with Giorgetta et al. (1999), our results suggest that this wave train emerges in response to the QBO modulation of convection over the tropical Indian Ocean in the preceding weeks.

The observed differences in the impact of the QBO on AM water vapour in July and August are consistent with the changes in the QBO signal on convection in these two months. In accordance with previous studies, we have observed that it is

https://doi.org/10.5194/egusphere-2023-1432
Preprint. Discussion started: 11 July 2023

convection, and associated temperature anomalies, over the southern flank of the AM that has the greatest impact on the moisture over the AM anticyclone. In turn, the QBO signal on convection in this region is linked to the modulation of convection over the equator. However, while in the period from mid-June to mid-July the signal over the southern flank of the AM occurs in response to the signal occurring simultaneously over the equator, from mid-July to August the equatorial signature strongly weakens and the signal over the southern flank of the AM seems to be associated with a Rossby wave train generated by equatorial convection in the previous weeks. The fact that the modulation of convection by the QBO occurs mainly over the region of the climatological maximum and only affects levels above 200hPa strongly suggests that the QBO needs the presence of significant convective activity to have an impact on the vertical extent of convection modulating atmospheric stability. Thus, as the climatological maximum of convection moves northward with the advance of summer and weakens at the equator (Fig. 9), the impact of the QBO on convection also weakens at equatorial latitudes. Comparison of the QBO response of convection (e.g., Fig. 7) to its seasonal shift (Fig. 9) shows that the QBO anomaly amplifies the climatological seasonal pattern.

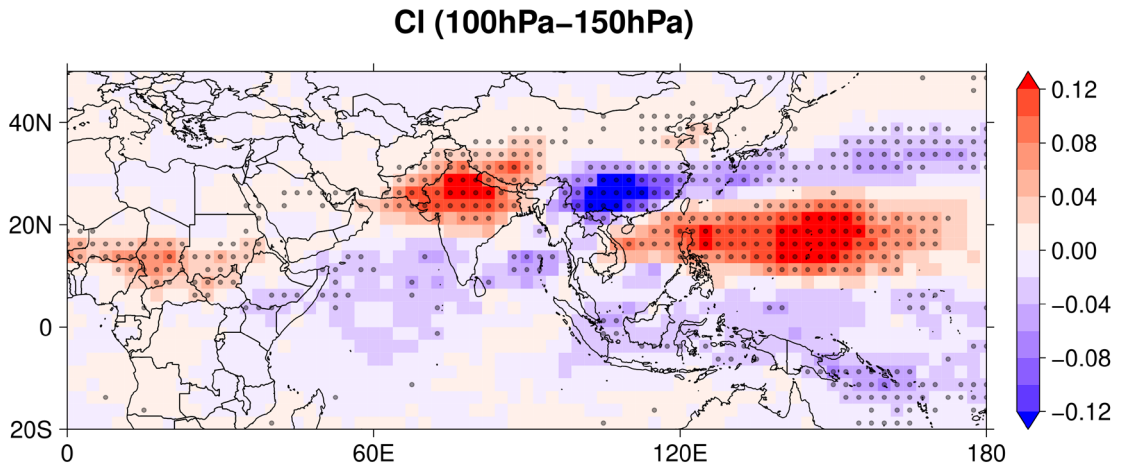

Figure 9: Difference between the climatological mean over the period 2005-2020 of the mean cloudiness between 100hPa and 150hPa corresponding to the time interval between 16 June and 16 July minus the average corresponding to the period 19 July - 18 August.

The cold anomaly over the equator associated with the QBO generates, in June-July, an intensification of convection in this region which, in turn, produces an anticyclonic Rossby gyre on the southern flank of the monsoon that increases convection in this area and causes a cooling that is counteracted by the warming associated with the secondary meridional circulation. In August, however, the cold anomaly over the equatorial region does not generate an intensification of convection. The modulation of convection over the southern flank of the AM is a response to a wave train generated by convection over the equator during June-July. However, the progressive weakening of the convection over the equator causes a weakening of the anomalies associated with the wave train over the tropical region so that, during the time window covering the second half of

https://doi.org/10.5194/egusphere-2023-1432
Preprint. Discussion started: 11 July 2023

July and the first half of August, the disturbance over the southern flank of the AM associated with this wave train is characterized by a cyclonic gyre that inhibits convection and causes a warm anomaly that moistens the AM.

Remarkaby, the general response of water vapour in the AM to variations in convection on both intra-seasonal and inter-annual time scales is very similar. Hence, the involved mechanisms, as detailed in this paper, could also help to explain changes in stratospheric water vapour in the AM region for convection changes in a changing climate. Follow-up studies on the climate change response of monsoon moisture will be a fruitful topic of future research.

https://doi.org/10.5194/egusphere-2023-1432
Preprint. Discussion started: 11 July 2023

Appendix A

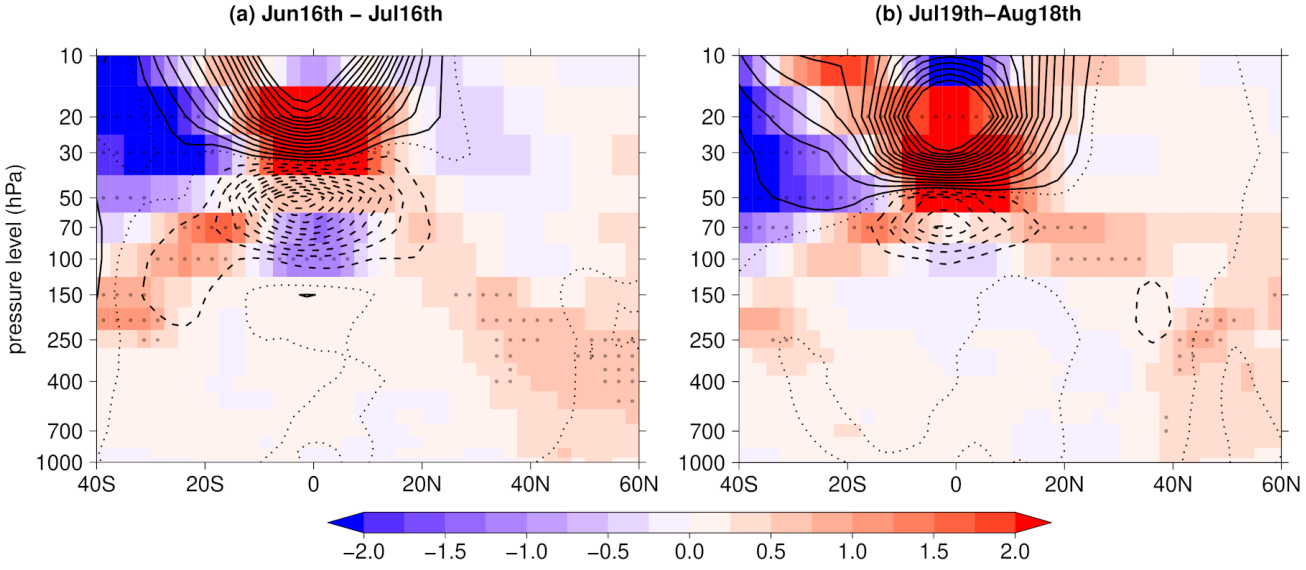

Figure A1: Latitude-height cross sections of QBO-W minus QBO-E differences for ERA5 global zoal mean of temperature (colors) and of zonal wind (black contours) averaged between June 16th and July 16th (a) and between July 19th and August 18th (b). In (a) diifferences correspond to the QBO index for July defined at 10hPa while for (b) we chose the QBO index defined at 20hPa for August. Solid/dashed contour lines show positive/negative anomalies with contour intervals at every 2m/s from 1m/s/-1m/s for positive/negative anomalies. Dots indicate significance at the 95% confidence level.

https://doi.org/10.5194/egusphere-2023-1432
Preprint. Discussion started: 11 July 2023

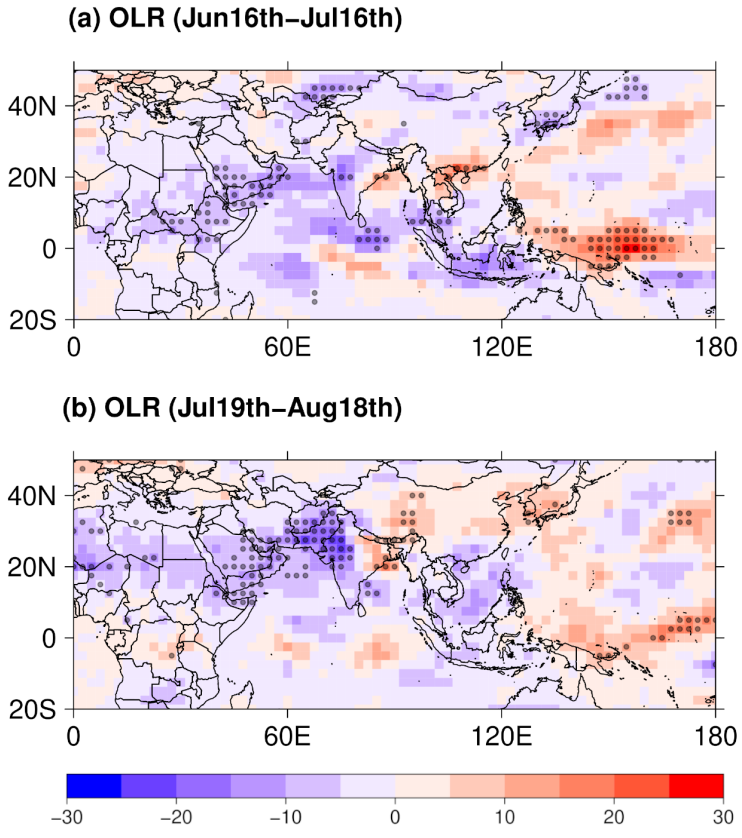

565

Figure A2: QBO-W minus QBO-E differences for OLR averaged between June 16th and July 16th (a) and between July 19th and August 19th (b). In (a) differences correspond to the QBO index for July defined at 10hPa while for (b) we chose the QBO index defined at 20hPa for August. Dots indicate significance at the 95% confidence level.

570

https://doi.org/10.5194/egusphere-2023-1432
Preprint. Discussion started: 11 July 2023

Data availability. MLS H_2O and Temperature version 4.2 data can be obtained from the MLS website https://mls.jpl.nasa.gov. The ERA5 data can be accessed through the Copernicus Climate Data Store website https://cds.climate.copernicus.eu/cdsapp#!/home.

Author contributions. CP and NP performed the data analysis. CP, NP, FP and DG contributed to the discussion of results. CP wrote the text. NP, FP and DG made the final review.

Competing interests. The authors declare that they have no conflict of interest.

Acknowledgements. This research was funded by the Spanish Ministerio de Economía y Competitividad through the project Variabilidad del Vapor de Agua en la Baja Estratosfera (CGL2016-78562-P).

References

Baldwin, M. P., Gray, L. J., Dunkerton, T. J., Hamilton, K., Haynes, P. H., Randel, W. J., Holton, J. R., Alexander, M. J., Hirota, I., Horinouchi, T., Jones, D. B., Kinnersley, J. S., Marquardt, C., Sato, K. and Takahashi, M.: The quasi-biennial oscillation, Reviews of Geophysics, 39(2), 179–229, doi:10.1029/1999rg000073, 2001.

Bannister, R. N., O'neill, A., Gregory, A. R., and Nissen, K. M.: The role of the south-east Asian monsoon and other seasonal features in creating the 'tape-recorder' signal in the Unified Model, Q.J.R. Meteorol. Soc., 130, 1531–1554, https://doi.org/10.1256/qj.03.106, 2004.

Brindley, H. E. and Harries, J. E.: The impact of far i.r. absorption on clear sky greenhouse forcing: sensitivity studies at high spectral resolution, Journal of Quantitative Spectroscopy and Radiative Transfer, 60, 151–180, https://doi.org/10.1016/s0022-4073(97)00152-0, 1998.

Collimore, C. C., Martin, D. W., Hitchman, M. H., Huesmann, A., and Waliser, D. E.: On The Relationship between the QBO and Tropical Deep Convection, J. Climate, 16, 2552–2568, https://doi.org/10.1175/1520-0442(2003)016<2552:otrbtq>2.0.co;2, 2003.

Dima, I. M., Wallace, J. M., and Kraucunas, I.: Tropical Zonal Momentum Balance in the NCEP Reanalyses, Journal of the Atmospheric Sciences, 62, 2499–2513, https://doi.org/10.1175/jas3486.1, 2005.

Dvortsov, V. L. and Solomon, S.: Response of the stratospheric temperatures and ozone to past and future increases in stratospheric humidity, J. Geophys. Res., 106, 7505–7514, https://doi.org/10.1029/2000jd900637, 2001.

Fueglistaler, S., Wernli, H., and Peter, T.: Tropical troposphere-to-stratosphere transport inferred from trajectory calculations, J. Geophys. Res., 109, n/a-n/a, https://doi.org/10.1029/2003jd004069, 2004.

https://doi.org/10.5194/egusphere-2023-1432
Preprint. Discussion started: 11 July 2023

Fueglistaler, S., Dessler, A. E., Dunkerton, T. J., Folkins, I., Fu, Q., and Mote, P. W.: Tropical tropopause layer, Rev. Geophys., 47, https://doi.org/10.1029/2008rg000267, 2009.

Fueglistaler, S. and Haynes, P. H.: Control of interannual and longer-term variability of stratospheric water vapor, J. Geophys. Res., 110, https://doi.org/10.1029/2005jd006019, 2005.

Geller, M. A., Zhou, X., and Zhang, M.: Simulations of the Interannual Variability of Stratospheric Water Vapor, J. Atmos. Sci., 59, 1076–1085, https://doi.org/10.1175/1520-0469(2002)059<1076:sotivo>2.0.co;2, 2002.

Gill, A. E.: Some simple solutions for heat-induced tropical circulation, Q.J Royal Met. Soc., 106, 447–462, https://doi.org/10.1002/qj.49710644905, 1980.

Giorgetta, M. A. and Bengtsson, L.: Potential role of the quasi-biennial oscillation in the stratosphere-troposphere exchange as found in water vapor in general circulation model experiments, J. Geophys. Res., 104, 6003–6019, https://doi.org/10.1029/1998jd200112, 1999.

Hersbach, H., Bell, B., Berrisford, P., Hirahara, S., Horányi, A., Muñoz-Sabater, J., Nicolas, J., Peubey, C., Radu, R., Schepers, D., Simmons, A., Soci, C., Abdalla, S., Abellan, X., Balsamo, G., Bechtold, P., Biavati, G., Bidlot, J., Bonavita, M., Chiara, G., Dahlgren, P., Dee, D., Diamantakis, M., Dragani, R., Flemming, J., Forbes, R., Fuentes, M., Geer, A., Haimberger, L., Healy, S., Hogan, R. J., Hólm, E., Janisková, M., Keeley, S., Laloyaux, P., Lopez, P., Lupu, C., Radnoti, G., Rosnay, P., Rozum, I., Vamborg, F., Villaume, S., and Thépaut, J.: The ERA5 global reanalysis, Q.J.R. Meteorol. Soc., 146, 1999–2049, https://doi.org/10.1002/qj.3803, 2020.

Holton, J. R. and Gettelman, A.: Horizontal transport and the dehydration of the stratosphere, Geophys. Res. Lett., 28, 2799–2802, https://doi.org/10.1029/2001gl013148, 2001.

Johnston, B. R., Xie, F., and Liu, C.: The Effects of Deep Convection on Regional Temperature Structure in the Tropical Upper Troposphere and Lower Stratosphere, JGR Atmospheres, 123, 1585–1603, https://doi.org/10.1002/2017jd027120, 2018.

Khaykin, S. M., Moyer, E., Krämer, M., Clouser, B., Bucci, S., Legras, B., Lykov, A., Afchine, A., Cairo, F., Formanyuk, I., Mitev, V., Matthey, R., Rolf, C., Singer, C. E., Spelten, N., Volkov, V., Yushkov, V., and Stroh, F.: Persistence of moist plumes from overshooting convection in the Asian monsoon anticyclone, Atmos. Chem. Phys., 22, 3169–3189, https://doi.org/10.5194/acp-22-3169-2022, 2022.

Konopka, P., Rolf, C., von Hobe, M., Khaykin, S. M., Clouser, B., Moyer, E., Ravegnani, F., D'Amato, F., Viciani, S., Spelten, N., Afchine, A., Krämer, M., Stroh, F., and Ploeger, F.: A long pathway of high water vapor from the Asian summer monsoon into the stratosphere, EGUsphere [preprint], https://doi.org/10.5194/egusphere-2023-498, 2023.

Lambert, A., Livesey, N., and Read, W.: MLS/Aura L2 Water Vapor (H2O) Mixing Ratio - Version 4, https://doi.org/10.5067/AURA/MLS/DATA2009, 2015.

Liang, C. K., Eldering, A., Gettelman, A., Tian, B., Wong, S., Fetzer, E. J., and Liou, K. N.: Record of tropical interannual variability of temperature and water vapor from a combined AIRS-MLS data set, J. Geophys. Res., 116, https://doi.org/10.1029/2010jd014841, 2011.

https://doi.org/10.5194/egusphere-2023-1432
Preprint. Discussion started: 11 July 2023

Liebmann B. and Smith, C.A.: Description of a Complete (Interpolated) Outgoing Longwave Radiation Dataset, Bulletin of the American Meteorological Society, 77, 1275-1277, 1996.

Livesey, N., Read, W., Wagner, P., Froidevaux, L., Lambert, A., Manney, G., Millán Valle, L., Pumphrey, H., Santee, M., Schwartz, M., Wang, S., Fuller, R., Jarnot, R., Knosp, B., Martinez, E., and Lay, R.: Version 4.2 × Level 2 data quality and description document, Jet Propul, Tech. rep., Lab., Tech. Rep. JPL D-33509 Rev. D, Pasadena, CA, USA, available at: https://mls.jpl.nasa.gov/data/v4-2_data_quality_document.pdf, 2020.

Matsuno, T.: Quasi-geostrophic motions in the equatorial area, J. Meteorol. Soc. Jpn., 44, 25–43, 1966.

Muhsin, M., Sunilkumar, S. V., Venkat Ratnam, M., Parameswaran, K., Krishna Murthy, B. V., and Emmanuel, M.: Effect of convection on the thermal structure of the troposphere and lower stratosphere including the tropical tropopause layer in the South Asian monsoon region, Journal of Atmospheric and Solar-Terrestrial Physics, 169, 52–65, https://doi.org/10.1016/j.jastp.2018.01.016, 2018.

Nützel, M., Podglajen, A., Garny, H., and Ploeger, F.: Quantification of water vapour transport from the Asian monsoon to the stratosphere, Atmos. Chem. Phys., 19, 8947–8966, https://doi.org/10.5194/acp-19-8947-2019, 2019.

Pahlavan, H. A., Fu, Q., Wallace, J. M., and Kiladis, G. N.: Revisiting the Quasi-Biennial Oscillation as Seen in ERA5. Part I: Description and Momentum Budget, Journal of the Atmospheric Sciences, 78, 673–691, https://doi.org/10.1175/jas-d-20-0248.1, 2021.

Park, M., Randel, W. J., Gettelman, A., Massie, S. T., and Jiang, J. H.: Transport above the Asian summer monsoon anticyclone inferred from Aura Microwave Limb Sounder tracers, J. Geophys. Res., 112, https://doi.org/10.1029/2006jd008294, 2007.

Peña-Ortiz, C., Manzini, E., and Giorgetta, M. A.: Tropical Deep Convection Impact on Southern Winter Stationary Waves and Its Modulation by the Quasi-Biennial Oscillation, Journal of Climate, 32, 7453–7467, https://doi.org/10.1175/jcli-d-18-0763.1, 2019.

Ploeger, F., Günther, G., Konopka, P., Fueglistaler, S., Müller, R., Hoppe, C., Kunz, A., Spang, R., Grooß, J.-U., and Riese, M.: Horizontal water vapor transport in the lower stratosphere from subtropics to high latitudes during boreal summer, J. Geophys. Res. Atmos., 118, 8111–8127, https://doi.org/10.1002/jgrd.50636, 2013.

Randel, W. J., Wu, F., Oltmans, S. J., Rosenlof, K., and Nedoluha, G. E.: Interannual Changes of Stratospheric Water Vapor and Correlations with Tropical Tropopause Temperatures, J. Atmos. Sci., 61, 2133–2148, https://doi.org/10.1175/1520-0469(2004)061<2133:icoswv>2.0.co;2, 2004.

Randel, W. J. and Park, M.: Deep convective influence on the Asian summer monsoon anticyclone and associated tracer variability observed with Atmospheric Infrared Sounder (AIRS), J. Geophys. Res., 111, https://doi.org/10.1029/2005jd006490, 2006.

Randel, W. J., Zhang, K., and Fu, R.: What controls stratospheric water vapor in the NH summer monsoon regions?, J. Geophys. Res. Atmos., 120, 7988–8001, https://doi.org/10.1002/2015jd023622, 2015.

https://doi.org/10.5194/egusphere-2023-1432
Preprint. Discussion started: 11 July 2023

Rosenlof, K. H., Tuck, A. F., Kelly, K. K., Russell, J. M., III, and McCormick, M. P.: Hemispheric asymmetries in water vapor and inferences about transport in the lower stratosphere, J. Geophys. Res., 102, 13213–13234, https://doi.org/10.1029/97jd00873, 1997.

Santee, M. L., Manney, G. L., Livesey, N. J., Schwartz, M. J., Neu, J. L., and Read, W. G.: A comprehensive overview of the climatological composition of the Asian summer monsoon anticyclone based on 10 years of Aura Microwave Limb Sounder measurements, J. Geophys. Res. Atmos., 122, 5491–5514, https://doi.org/10.1002/2016jd026408, 2017.

Stenke, A. and Grewe, V.: Simulation of stratospheric water vapor trends: impact on stratospheric ozone chemistry, Atmos. Chem. Phys., 5, 1257–1272, https://doi.org/10.5194/acp-5-1257-2005, 2005.

Tian, E. W., Su, H., Tian, B., and Jiang, J. H.: Interannual variations of water vapor in the tropical upper troposphere and the lower and middle stratosphere and their connections to ENSO and QBO, Atmos. Chem. Phys., 19, 9913–9926, https://doi.org/10.5194/acp-19-9913-2019, 2019.

Waters, J., Froidevaux, L., Harwood, R., Jarnot, R., Pickett, H., Read, W., Siegel, P., Cofield, R., Filipiak, M., Flower, D., Holden, J., Lau, G., Livesey, N., Manney, G., Pumphrey, H., Santee, M., Wu, D., Cuddy, D., Lay, R., Loo, M., Perun, V., Schwartz, M., Stek, P., Thurstans, R., Boyles, M., Chandra, K., Chavez, M., Chen, G.-S., Chudasama, B., Dodge, R., Fuller, R., Girard, M., Jiang, J., Jiang, Y., Knosp, B., LaBelle, R., Lam, J., Lee, K., Miller, D., Oswald, J., Patel, N., Pukala, D., Quintero, O., Scaff, D., Van Snyder, W., Tope, M., Wagner, P., and Walch, M.: The earth observing system microwave limb sounder (EOS MLS) on the Aura satellite, IEEE T. Geosci. Remote, 44, 1075–1092, 2006.

Wright, J. S., Fu, R., Fueglistaler, S., Liu, Y. S., and Zhang, Y.: The influence of summertime convection over Southeast Asia on water vapor in the tropical stratosphere, J. Geophys. Res., 116, https://doi.org/10.1029/2010jd015416, 2011.

Yao, B., Teng, S., Lai, R., Xu, X., Yin, Y., Shi, C., and Liu, C.: Can atmospheric reanalyses (CRA and ERA5) represent cloud spatiotemporal characteristics?, Atmospheric Research, 244, 105091, https://doi.org/10.1016/j.atmosres.2020.105091, 2020.

Zhang, K., Fu, R., Wang, T., and Liu, Y.: Impact of geographic variations of the convective and dehydration center on stratospheric water vapor over the Asian monsoon region, Atmos. Chem. Phys., 16, 7825–7835, https://doi.org/10.5194/acp-16-7825-2016, 2016.

Zhou, X. L., Geller, M. A., and Zhang, M.: Temperature Fields in the Tropical Tropopause Transition Layer, J. Climate, 17, 2901–2908, https://doi.org/10.1175/1520-0442(2004)017<2901:tfittt>2.0.co;2, 2004.

Zhou, X.-L., Geller, M. A., and Zhang, M.: Cooling trend of the tropical cold point tropopause temperatures and its implications, J. Geophys. Res., 106, 1511–1522, https://doi.org/10.1029/2000jd900472, 2001.